

Coherent Anti-Stokes Raman Spectroscopy of Highly Compressed Solid Deuterium at 300 K: Evidence for a New Phase and Implications for the Band Gap

Bruce J. Baer, William J. Evans, and Choong-Shik Yoo

H-Division, Physics & Advanced Technologies, Lawrence Livermore National Laboratory, Livermore, California 94550, USA

(Received 19 January 2007; published 8 June 2007)

Coherent anti-Stokes Raman spectroscopy has been used to study deuterium at ambient temperature to 187 GPa, the highest pressure this technique has ever been applied. The pressure dependence of the ν_1 vibron line shape indicates that deuterium has a $\rho_{\text{direct}} = 0.501$ and $\rho_{\text{exciton}} = 0.434$ mol/cm³ for a band gap of $2\omega_p = 4.66$ eV. The extrapolation from the ambient pressure band gap yields a metallization pressure of 460 GPa, confirming earlier measurements. Above 143 GPa, the Raman shift data provide clear evidence for the presence of the *ab initio* predicted I' phase of deuterium.

DOI: [10.1103/PhysRevLett.98.235503](https://doi.org/10.1103/PhysRevLett.98.235503)

PACS numbers: 62.50.+p, 42.65.Dr, 71.20.-b

Understanding the high-pressure properties of hydrogen and its isotopes is of fundamental importance to condensed matter physics [1–4] and planetary modeling [5]. Though the simplest of molecules, due to its quantum nature, solid H₂ has been predicted to give rise to many interesting properties such as high-temperature superconductivity [2]. A recent study found no evidence for a metallic phase of solid hydrogen up to 320 GPa [6], but predicted a band gap closure at 450 GPa on the basis of absorption measurements on a sample that began to darken near 300 GPa. Another study [7] claims that hydrogen is still transparent at 342 GPa. These contradictory observations have been suggested to be a result of diverging pressure calibrations above 150 GPa [8]. Interestingly, electrical measurements of shock-compressed fluid D₂ at 140 GPa and ~3000 K show high conductivity [9]. In fact, the determination of the band gap of H₂ with diamond-anvil cells (DACs) using linear spectroscopies is challenging, if not limited, because of the restrictions inherent with the diamond's opacity [10] and strain-induced fluorescence [11].

The high-pressure behavior of H₂ and D₂ has been extensively explored, both computationally and experimentally in recent years [12–24], yielding a wealth of information at high pressures but typically limited to temperatures below 150 K. Three phases of solid H₂ (and D₂) have been identified: the symmetric phase (SP or phase I) [13] with an isotropic rotational state, the broken symmetry phase (BSP or phase II) [14] with orientational order of molecules in the spherically symmetric even J states, and the A phase (phase III) with dramatically enhanced IR oscillator strength [15]. For D₂, these three phases meet at the I-II-III triple point near 160 GPa and 130 K [16]. Recent evidence indicates that the orientational ordering transition from phase I to II occurs with a small discontinuity in specific volume [22]; however, the phase boundary exhibits a strong isotope shift (28 GPa in *o*-D₂, 110 GPa in *p*-H₂, and 69 GPa in HD, near 5 K) [14,17,18], owing to strong quantum effects. The phase II to III transition occurs with a large discontinuous drop in the Raman vibron

frequency, ~ 100 cm⁻¹ for D₂ at 77 K [15]. The Raman shift discontinuity between phase II (I, or possibly I', above the triple point) and III gradually decreases with increasing temperature and eventually vanishes at the critical point near 165 GPa and 150 K for H₂ [19], but for D₂ this occurs at a much higher pressure and temperature [20]. There is significant electron-phonon coupling at these pressures [15], which can be interpreted as the result of a charge-transfer (CT) pairing of molecules in phase III [21]. Recent path-integral Monte Carlo simulations predict that for D₂ phase I transforms to a new orientationally ordered phase I' above 145 GPa at ambient temperature [12].

Experimentally, optical spectroscopy at ultrahigh pressures is difficult due to intense strain-induced diamond fluorescence competing with a relatively weak Raman signal from the sample as well as the diminishing luminescence of the ruby pressure sensor. Hydrogen is highly compressible, resulting in extremely small samples with a significant change in optical band gap. Furthermore, the absorption edge of diamond is moving down below 3 eV at ultrahigh pressures [10] so that optical studies under these conditions must compete against the narrowing transparency of the diamond window.

To overcome these limitations inherent with the diamond's opacity and strain-induced fluorescence, we have employed a multiphoton method, coherent anti-Stokes Raman spectroscopy (CARS) [25]. CARS can be used to probe energy states significantly above the diamond window cutoff. This method uses two laser pulses set at ω_p and ω_s such that $\omega_p - \omega_s$ is resonant with the molecular vibration under study. Broadband CARS simply uses a spectrally broad ω_s . The emission occurs at $2\omega_p - \omega_s$. The presence of electronic states near $2\omega_p$ will affect the CARS line shape. Since the diamond can be transparent to ω_p (as well as $2\omega_p - \omega_s$), but not $2\omega_p$, this opens up the possibility of studying samples at energies well above the diamond cutoff. CARS also has the benefit of having no background fluorescence, since the emission is blueshifted from the excitation pulses. In this Letter, we present the

accurate determination of the band gap at $2\omega_p$ as well as the experimental evidence for a new phase (I') of D_2 appearing above 143 GPa at 300 K.

For experiments, D_2 gas (>99.9% pure, ~ 0.2 GPa) was loaded into a membrane DAC using a high-pressure gas-loading device. Samples were initially ~ 30 μm in diameter at low pressures. Pressures were measured using ruby luminescence [23] and/or the Raman shift of diamond [26] with an error of no more than 3 GPa. Broadband CARS spectra were obtained using a system that utilized a mode-locked Q -switched Nd:YAG laser to generate a frequency doubled pulse at 532 nm (120 ps) and a synchronously pumped, spectrally broad, dye laser pulse from 625 to 645 nm (30 to 50 ps). The two pulses are overlapped both spatially and temporally at the sample. Pulse energies of less than 5 μJ were used to prevent diamond breakage. The laser repetition rate is approximately 1 kHz, and the CARS spectra were signal averaged for up to 30 min.

All CARS experiments yielded spectra with an extremely high signal to noise ratio and had essentially zero luminescence background, as shown in Fig. 1. Spectral line shape analyses [25] in the absence of any significant inhomogeneous broadening can be performed

using Eq. (1).

$$I_{as} \propto I_s \left[\left(\sum_j \frac{\Gamma_j \chi_j^{\text{pk}} (\omega_j - \omega_p + \omega_s)}{(\omega_j - \omega_p + \omega_s)^2 + \Gamma_j^2} + \chi^{\text{nr}} \right)^2 + \left(\sum_j \frac{\Gamma_j^2 \chi_j^{\text{pk}}}{(\omega_j - \omega_p + \omega_s)^2 + \Gamma_j^2} \right)^2 \right]. \quad (1)$$

The subscripts s , as , and p refer to Stokes, anti-Stokes, and pump frequencies, respectively. χ^{pk} and χ^{nr} are the resonant and nonresonant third-order polarizabilities. Γ_j is the half-width at half-maximum intensity. The subscript j refers to each vibrational mode. This formula yields the energy, linewidth, and ratio of the third-order polarizabilities of the resonant versus nonresonant contributions to the CARS signal of the Raman active vibration. Fitting to this formula yielded extremely accurate peak positions, linewidths, and χ ratios, as shown in Fig. 1 (red line).

CARS spectra contain both resonant and nonresonant contributions, as evidenced in Eq. (1) and schematically represented in the center panel of Fig. 1. The resonant process [the second summation term of Eq. (1)] occurs when the energy difference of the two colors (ω_p and ω_s) coherently stimulate the molecular vibration at the beat frequency. For this experiment ω_p is the frequency doubled Nd:YAG, 532.07 nm. An additional photon of ω_p can stimulate emission of the vibrationally excited molecule at the sum frequency of ω_p plus the vibrational energy ($\omega_p - \omega_s$) in the short time before the coherently excited molecule dephases. In the nonresonant process, two photons of ω_p are virtually absorbed while an additional photon at ω_s is created as emission along with a photon at $2\omega_p - \omega_s$. For H_2 (or D_2) at low pressure, there is no electronic energy level near $2\omega_p$, so the contribution from the nonresonant process is almost negligible. However, as the pressure is increased, the exciton and, eventually, the direct band gap will approach $2\omega_p$ thus increasing the contribution from the nonresonant third-order polarizability: χ^{nr} . The enhancement of the nonresonant term due to this pressure tuning is apparent in the line shape analysis as demonstrated in Fig. 1.

To determine the density corresponding to a band gap of $2\omega_p = 4.66$ eV, a plot of $\chi^{\text{nr}}/\chi^{\text{pk}}$ as a function of density is presented in Fig. 2. Densities are calculated using a previously obtained equation of state [22]. The shoulder at lower density corresponds to the exciton. The optical CARS approach that we have used is sensitive to any energy level that is resonant with the virtual level accessed by the pump beams. The optical CARS technique restricts the probe to k space near the Brillouin zone center, making it more likely that we measure the exciton level rather than the indirect gap. This first resonance in Fig. 2, at a density of 0.434 mol/cm³ (162 GPa), closely coincides with the previously reported value [6,24] for a band gap energy of 4.66 eV. The second resonance, interpreted to be the direct band gap, is projected to occur at a density of

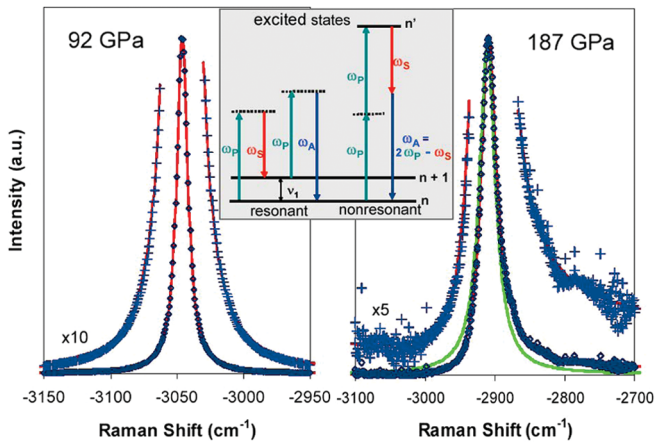


FIG. 1 (color). Representative CARS spectra of D_2 demonstrating the contribution of the third-order nonresonant polarizability to line shape: Left panel: D_2 vibron at 92 GPa and 300 K, showing a negligible contribution from χ^{nr} . The diamonds represent the raw data after it has been normalized for dye laser intensity. The best fit (red line) of the data to Eq. (1) yields the spectral parameters $\nu = 3046$ cm^{-1} , $\Gamma_{\text{FWHM}} = 10.1$ cm^{-1} , and $\chi^{\text{nr}}/\chi^{\text{pk}} = 0.0028$. Right panel: D_2 vibron at 187 GPa and 300 K, clearly showing a significant asymmetric spectral line shape. The best fit (red line) yields $\nu = 2910.6$ cm^{-1} , $\Gamma_{\text{FWHM}} = 27.3$ cm^{-1} , and $\chi^{\text{nr}}/\chi^{\text{pk}} = 0.086$. For comparison, an equivalent spectrum having $\chi^{\text{nr}} = 0$ is also overlaid (green line.) The small dips in the spectral data near 2720 and 2810 cm^{-1} are an artifact arising from fitting the dye laser spectrum over such a large region. Center panel: A schematic representation is diagrammed for the two dominant, resonant and nonresonant, processes contributing to the CARS spectral line shape. The corresponding third-order polarizabilities are, respectively, χ^{pk} and χ^{nr} from Eq. (1).

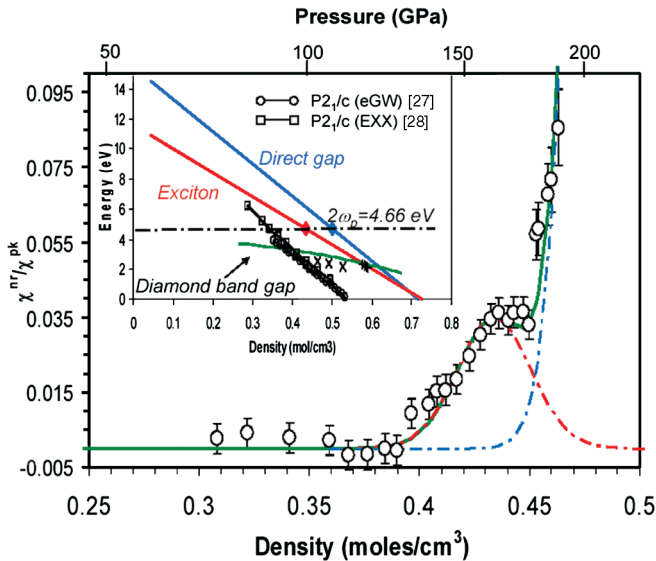


FIG. 2 (color). The ratio of third-order nonresonant to resonant polarizabilities (χ^{nr}/χ^{pk}) plotted as a function of density when $2\omega_p = 4.66$ eV. The data are fit assuming a Gaussian line shape for the direct band gap (blue dot-dash line) and exciton (red dot-dash line) with equal linewidth, which was determined to be 0.033 mol/cm³. The sum of these two processes is in green. The peak corresponding to the exciton is centered at 0.434 mol/cm³ (162 GPa) and the direct band gap at 0.501 mol/cm³ (223 GPa). From this fit, the intensity of the direct band gap peak is 40 times that of the exciton peak. Inset: The band gap of D_2 measured in the present study in comparison with some theoretically predicted band gap closures [27,28] (eGW: empirically corrected band gaps, EXX: exact-exchange calculations) and those determined experimentally [6] by resonance Raman (\times symbol) and absorption spectroscopy (+ symbol.) The diamond window cut-off is shown in green [10]. The direct band gap (blue line) and exciton (red line) are extrapolated from the ambient pressure values [24] through the corresponding $2\omega_p = 4.66$ eV point to nearly the same density of 0.72 mol/cm³ or 460 GPa for metallization.

0.501 mol/cm³ (223 GPa) by assuming the resonance has the same linewidth of 0.033 mol/cm³ as the first resonance in the Fig. 2 plot. A simple linear extrapolation of the direct band gap and the exciton has them intersect near a metallization density of ~ 0.72 mol/cm³, or 460 GPa. This is a remarkable independent confirmation of the results from an earlier study [6] using data obtained at pressures more than 100 GPa below the absorption measurements.

Evidence for a new phase, derived from the pressure-dependent vibron energy of D_2 using CARS, is apparent. Figure 3(a) summarizes the pressure dependence of the Raman shift of D_2 at 300 K by CARS in comparison with that previously determined by classical Raman spectroscopy at 77 K [14,18]. It shows that the vibron frequency at 300 K gradually shifts away from those of phase I and II at 77 K and approaches that of phase III at 77 K. Furthermore, unlike the 77 K data, the data at 300 K reveal an abrupt change in the rate of the pressure-dependent Raman shift

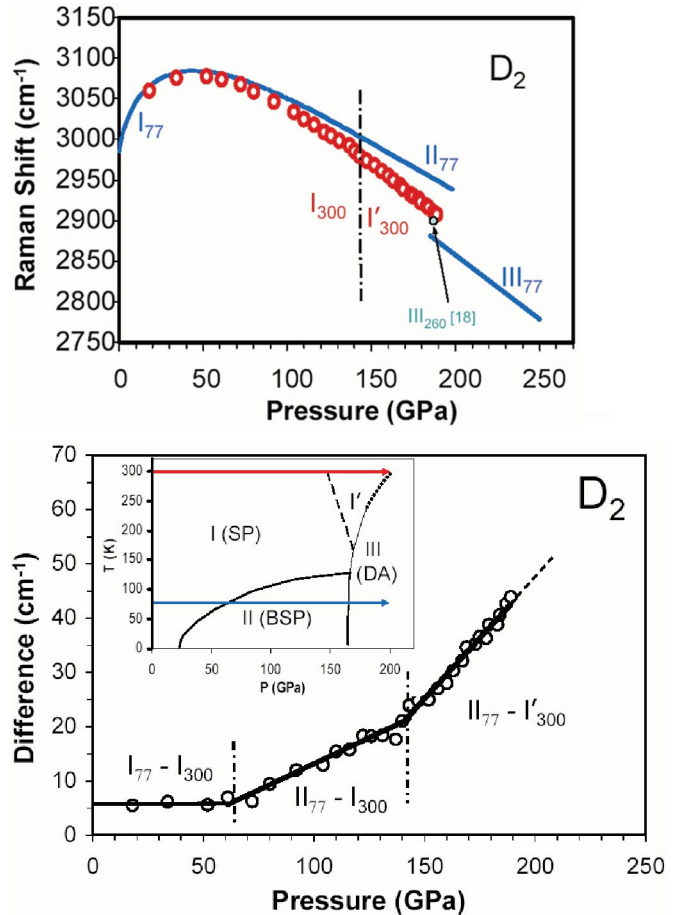


FIG. 3 (color). (a) Pressure dependence of the Raman shift of the D_2 vibron obtained from the present CARS experiments at 300 K (red circles), in comparison with those obtained by ordinary Raman spectra at 77 K (blue lines) calculated from Ref. [18]. Subscripts refer to temperature in Kelvins. The large discontinuous change at 77 K is due to the transition from phase II to III. A small change of the pressure-dependent shift rate (dv/dP) at 143 GPa and 300 K is due to the transition from phase I (SP) to phase I'. (b) The difference in Raman shift between the D_2 vibrons measured at 77 K (Ref. [18]) and 300 K (this Letter) as a function of pressure. Changes in slope occur at 62 and 143 GPa. The lines are fit using least linear square of the data in each region. Below 62 GPa the slope is near zero. The errors associated with the measurements are $\sim 2\%$ in pressure and ~ 2 cm⁻¹ in Raman shift. The slopes above and below 143 GPa are 0.193 and 0.448 cm⁻¹/GPa, respectively. Inset: Phase diagram of o - D_2 adapted from Ref. [12]. The two temperature paths (77 K in blue, 300 K in red) are diagrammed for comparison. The observed slope change at 143 GPa occurs at the onset of the phase I-to-I' transition.

near 143 GPa, which is especially apparent in the difference plot in Fig. 3(b). At low pressures, the difference in Raman shift is due to the temperature dependence of the vibron in phase I, which appears to have virtually no pressure dependence. The first deviation in slope occurs at 62 GPa, due to the transition to the BSP phase at 77 K [17]. The second deviation at 143 GPa, however, arises

from a transition at 300 K, as it is compared to the BSP phase at 77 K. In fact, the transition pressure of 143 GPa is very close to the I-to-I' transition pressure calculated for pure *o*-D₂ [see the Fig. 3(b) inset] [12]. The spectral linewidth, which generally increased with pressure, also shows a dip in that trend at the transition pressure. The increasingly larger difference above 143 GPa is not surprising given the large discontinuity in Raman shift between phases II to III observed at 77 K. In fact, the Raman shift of phase I' at 187 GPa and 300 K, 2910 cm⁻¹, is nearly the same as that of phase III, 2900 cm⁻¹, at the onset of the I to III transition near 186 GPa and 260 K [20]. This suggests that the phase III vibron has a much larger temperature dependence than phase I. Therefore, the present study supplies additional evidence that the transition observed above the critical point [20] at ~171 GPa is from phase I' to III, rather than from phase I to III and, combining the two results, the stability field of phase I' at 300 K can now be bracketed between 143 and 200 GPa, as shown in the inset of Fig. 3(b).

The present study offers evidence for a new phase (I') of D₂ at pressures from 143 to 190 GPa at 300 K. The direct band gap at these pressures is still large, >5 eV, so that the I-I' phase transition is not solely an orientational ordering transition, as predicted by *ab initio* calculations [12]. Furthermore, it is likely that the extent of orientational ordering in D₂ increases over a widening pressure range with increasing temperature. Phase I' is bounded below by phase I, rotationally disordered states at the transition pressure, 143 GPa, and then gradually orders to one having a configuration of D₂ pairs which allow for CT states [21] near 200 GPa, phase III. This implies that the suggested critical point of D₂ near 165 GPa and 170 K is in fact a triple point, as noted previously [20]. Thus the ordering process in phase I' occurs over an increasingly larger pressure range as the temperature is increased (i.e., classical ordering arising from ΔS), in contrast to a similar ordering process of phase II which occurs over the larger pressure range at the lower temperature (i.e., quantum ordering). Therefore, this critical or triple point seems to signify the temperature above which D₂ behaves more classically.

The present study was performed in support of the LDRD Program (No. 05-ERD-036) at Lawrence Livermore National Laboratory, University of California, under the auspices of the U.S. Department of Energy under Contract No. W-7405-Eng-48.

-
- [1] E. Wigner and H. B. Huntington, J. Chem. Phys. **3**, 764 (1935).
 [2] N. W. Ashcroft, Phys. Rev. Lett. **21**, 1748 (1968); J. Phys. Condens. Matter **12**, A129 (2000).
 [3] H. K. Mao and R. J. Hemley, Rev. Mod. Phys. **66**, 671 (1994).

- [4] I. F. Silvera, Rev. Mod. Phys. **52**, 393 (1980).
 [5] W. J. Nellis, S. T. Weir, and A. C. Mitchell, Science **273**, 936 (1996).
 [6] P. Loubeyre, F. Occelli, and R. LeToullec, Nature (London) **416**, 613 (2002).
 [7] C. Narayna, H. Luo, J. Orloff, and A. L. Ruoff, Nature (London) **393**, 46 (1998).
 [8] A. D. Chijioke, W. J. Nellis, A. Soldatov, and I. F. Silvera, J. Appl. Phys. **98**, 114905 (2005).
 [9] S. T. Weir, A. C. Mitchell, and W. J. Nellis, Phys. Rev. Lett. **76**, 1860 (1996).
 [10] A. L. Ruoff, H. Luo, and Y. K. Vohra, J. Appl. Phys. **69**, 6413 (1991).
 [11] Y. K. Vohra, H. Xia, H. Luo, and A. L. Ruoff, Appl. Phys. Lett. **57**, 1007 (1990); H. K. Mao and R. J. Hemley, Nature (London) **351**, 721 (1991).
 [12] M. P. Surh, K. J. Runge, T. W. Barbee, E. L. Pollock, and C. Mailhot, Phys. Rev. B **55**, 11 330 (1997).
 [13] A. F. Schuch and R. L. Mills, Phys. Rev. Lett. **16**, 616 (1966); H. K. Mao, A. P. Jephcoat, R. J. Hemley, L. W. Finger, C. S. Zha, R. M. Hazen, and D. E. Cox, Science **239**, 1131 (1988).
 [14] H. E. Lorenzana, I. F. Silvera, and K. A. Goettel, Phys. Rev. Lett. **64**, 1939 (1990); Phys. Rev. Lett. **63**, 2080 (1989).
 [15] R. J. Hemley and H. K. Mao, Phys. Rev. Lett. **61**, 857 (1988); Phys. Rev. Lett. **63**, 1393 (1989); M. Hanfland, R. J. Hemley, and H. K. Mao, Phys. Rev. Lett. **70**, 3760 (1993).
 [16] L. Cui, N. H. Chen, S. J. Jeon, and I. F. Silvera, Phys. Rev. Lett. **72**, 3048 (1994).
 [17] I. F. Silvera and R. J. Wijngaarden, Phys. Rev. Lett. **47**, 39 (1981).
 [18] F. Moshary, N. H. Chen, and I. F. Silvera, Phys. Rev. B **48**, 12613 (1993).
 [19] R. J. Hemley and H. K. Mao, Science **249**, 391 (1990); K. J. Runge, M. P. Surh, C. Mailhot, and E. L. Pollock, Phys. Rev. Lett. **69**, 3527 (1992); L. Cui, N. H. Chen, and I. F. Silvera, Phys. Rev. B **51**, 14 987 (1995).
 [20] A. F. Goncharov, I. I. Mazin, J. H. Eggert, and R. J. Hemley, H. K. Mao, Phys. Rev. Lett. **75**, 2514 (1995).
 [21] R. J. Hemley, Z. G. Soos, M. Hanfland, and H. K. Mao, Nature (London) **369**, 384 (1994).
 [22] I. Goncharenko and P. Loubeyre, Nature (London) **435**, 1206 (2005); P. Loubeyre, R. LeToullec, D. Hausermann, M. Hanfland, R. J. Hemley, H. K. Mao, and L. W. Finger, Nature (London) **383**, 702 (1996).
 [23] H. K. Mao, J. Xu, and P. M. Bell, J. Geophys. Res. **91**, 4673 (1986).
 [24] R. J. Hemley, M. Hanfland, and H. K. Mao, Nature (London) **350**, 488 (1991).
 [25] B. J. Baer and C.-S. Yoo, Rev. Sci. Instrum. **76**, 013907 (2005).
 [26] F. Occelli, P. Loubeyre, and R. LeToullec, Nat. Mater. **2**, 151 (2003).
 [27] K. A. Johnson and N. W. Ashcroft, Nature (London) **403**, 632 (2000).
 [28] M. Stadele and R. M. Martin, Phys. Rev. Lett. **84**, 6070 (2000).